Band structures in highly strained 3D nanowires

Y. Hadjimichael*, O. Marquardt*, C. Merdon*, P. Farrell*
* Weierstrass Institute (WIAS), Mohrenstr. 39, 10117 Berlin, Germany

Email: yiannis.hadjimichael@wias-berlin.de

***Abstract*—We mathematically derive a new nonlinear strain model to simulate the conduction and valence bands in highly bent 3D hexagonal nanowires with GaAs core and asymmetric ($Al_\alpha In_{1-\alpha}$)As stressor. The model is based on a transformation of the 1st Piola-Kirchhoff stress tensor and an appropriate energy functional that captures the dynamics of the induced strain due to lattice number mismatch. Finally, we solve PDE model via the finite element method and use the strain profiles as input to a $\mathbf{k}\cdot\mathbf{p}$ simulation tool to compute the energy bands.**

I. Introduction

Nanowires are of great interest for many applications such as optoelectronics, solar cells, and sensors. For instance, nanowires may reduce the amount of silicon in solar cells [1]. Here, we study the strain effects in drastically bent hexaogonal zincblende nanowires due to a asymmetrically lattice-mismatched core and stressor. Experiments show that the strain heavily deforms the nanowires [2]. We propose a non-linear PDE model that captures the experimentally shown large finite-strain elastic deformation (up to 180°) and solve it numerically via the finite element method. Finally, we compute the band energy profiles on a cross section by using the $\mathbf{k}\cdot\mathbf{p}$ approach implemented in the `SPHInX` software [4].

II. Modelling strain in bent nanowires

We consider a heterostructured nanowire. The hexagonal core region is composed of GaAs and the second region consists of an ($Al_\alpha In_{1-\alpha}$)As alloy that covers the half side of the structure and acts as a stressor, see Figure 1a. Due to the lattice number mismatch between both materials, strain across the interface leads to a large deformation (see Figure 1b).

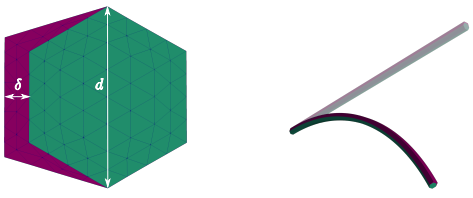

(a) Cross section (b) Unbent/bent wire

Fig. 1. Hexagonal nanowire consisting of bulk GaAs (green region). The nanowire is coated on one side (purple region) by a ($Al_\alpha In_{1-\alpha}$)As stressor. The length of the nanowire is set to $L = 2000$ nm, the diameter of the core is $d = 50$ nm, and the thickness of the stressor region is $\delta = 6.5$ nm.

Let $\bar{\Omega}$ be the closure of the open and connected set $\Omega \subset \mathbb{R}^3$ containing stressor and core. We call $\bar{\Omega}$ the *reference (Lagrangian) configuration* (initial volume before deformation), $\boldsymbol{\phi} : \bar{\Omega} \to \mathbb{R}^3$ the *deformation*, and $\boldsymbol{u} : \bar{\Omega} \to \mathbb{R}^3$ the *displacement* of the reference configuration. That is, $\boldsymbol{\phi}(\boldsymbol{x}) = \boldsymbol{x} + \boldsymbol{u}(\boldsymbol{x})$, where $\boldsymbol{x} \in \bar{\Omega}$ is the *Lagrangian variable*. We assume no applied body or surface forces are acting on the nanowire; thus, we can model the deformation by considering the following equilibrium system in the reference configuration [6]

$$-\operatorname{div}(\boldsymbol{T}(\boldsymbol{x})) = \mathbf{0}, \quad \forall \boldsymbol{x} \in \Omega, \tag{1a}$$

$$\boldsymbol{T}(\boldsymbol{x})\boldsymbol{n} = \mathbf{0}, \quad \forall \boldsymbol{x} \in \partial\Omega, \tag{1b}$$

where $\boldsymbol{T}$ the 1st Piola–Kirchhoff stress tensor, and $\boldsymbol{n}$ is the unitary normal vector to $\partial\Omega$. Considering an energy-based approach, the tensor $\boldsymbol{T}$ can be implicitly defined by the *stored energy function* $\widehat{W} : \bar{\Omega} \times \mathbb{M}^3_+ \to \mathbb{R}$ as

$$\boldsymbol{T}(\boldsymbol{x}) = \frac{\partial \widehat{W}(\boldsymbol{x}, \boldsymbol{F})}{\partial \boldsymbol{F}}, \quad \text{for all } \boldsymbol{x} \in \bar{\Omega}, \tag{2}$$

where $\boldsymbol{F} \coloneqq \nabla\boldsymbol{\phi} = \boldsymbol{I} + \nabla\boldsymbol{u}$ is the deformation gradient. It can be shown that the stored energy function is given by

$$\widehat{W}(\boldsymbol{x}, \boldsymbol{F}) = \det(\boldsymbol{M}) W(\boldsymbol{x}, \boldsymbol{F}\boldsymbol{M}^{-1}). \tag{3}$$

The matrix $\boldsymbol{M}(\boldsymbol{x}) = \boldsymbol{I} + \boldsymbol{\varepsilon}_0(\boldsymbol{x})$ describes the *prestrain* and is the driving force of the deformation. It is is expressed in terms of the *equilibrium strain tensor* $\boldsymbol{\varepsilon}_0$, which depends on the material's lattice number. Hence, the equilibrium strain is different in each region of the composite structure. We define $\boldsymbol{\varepsilon}_0 \coloneqq a(\boldsymbol{x})\boldsymbol{I}$, where $a(\boldsymbol{x}) = (l(\boldsymbol{x}) - l_{\text{ref}})/l(\boldsymbol{x})$ is the relative error of the lattice number of each material and l_{ref} denotes the volumetric average lattice number of the nanowire. Finally, by assuming a non-linear Green–St-Venant strain tensor $\boldsymbol{\varepsilon} \coloneqq (\boldsymbol{F}^\mathsf{T}\boldsymbol{F} - \boldsymbol{I})/2$, we choose the function W in (3) to be $W(\boldsymbol{x}, \boldsymbol{F}) = \frac{1}{8}(\boldsymbol{F}^\mathsf{T}\boldsymbol{F} - I) : \mathbf{C}(\boldsymbol{F}^\mathsf{T}\boldsymbol{F} - I)$, where $\mathbf{C} \in \mathbb{R}^{3\times3\times3\times3}$ is the fourth-order *elasticity tensor*. This choice yields $\boldsymbol{T}(\boldsymbol{x}) = \boldsymbol{F}\,\mathbf{C}\,\boldsymbol{\varepsilon}$ in the case that $\boldsymbol{M}(\boldsymbol{x}) = \boldsymbol{I}$, i.e., all regions of the nanowire consist of the same material. Now, using (2) and (3) we can rewrite equation (1a) the

$$-\operatorname{div}\left(\frac{1}{1 + a(\boldsymbol{x})}\boldsymbol{F}\,\mathbf{C}\,\tilde{\boldsymbol{\varepsilon}}(\boldsymbol{u})\right) = \mathbf{0}, \tag{4}$$

where $\tilde{\boldsymbol{\varepsilon}}(\boldsymbol{u}) = \boldsymbol{\varepsilon}(\boldsymbol{x}) - a(\boldsymbol{x})\,(1 + a(\boldsymbol{x})/2)\,\boldsymbol{I}$. The model (4) is solved with Dirichlet boundary conditions on a fixed side and homogeneous Neumann boundary conditions on the other edges. We used the Julia finite element package `GradientRobustMultiPhysics.jl`.

978-1-6654-7899-1/22/$31.00 ©2022 IEEE

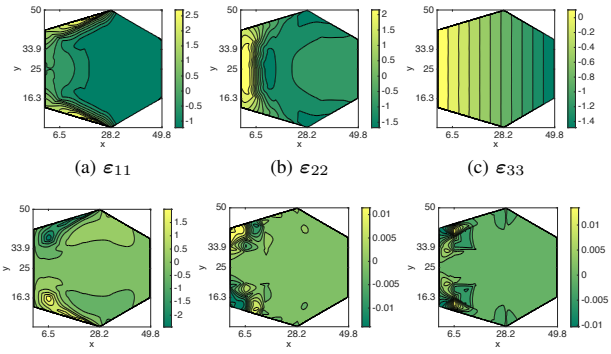

(a) ε_{11} (b) ε_{22} (c) ε_{33}

(d) ε_{12} (e) ε_{23} (f) ε_{33}

Fig. 2. Strain components computed on a cross section at $L = 1000$ nm.

III. Simulation Results for Band Structures

We compute the band-edge energies on a cross section of the nanowire perpendicular to the bending axis with an eight-band $\mathbf{k} \cdot \mathbf{p}$ model for zincblende semiconductors [5]. We use the generalized multiband $\mathbf{k} \cdot \mathbf{p}$ module of the plane wave-based `SPHInX` library, where we used the previously computed strain profile as input. The parameters are in [3].

Figure 2 shows the six upper elements of the symmetric strain tensor computed on a cross section at half the length of a GaAs/($Al_{0.7}In_{0.3}$)As nanowire. The diagonal elements are dominant with ε_{22} to be significantly larger in the stressor and $\varepsilon_{11} \approx \varepsilon_{22}$ in the core region. Thus, we conclude that the strain resembles a uniaxial tensile strain in the stressor region and biaxial compressive strain in the core region. Similar behavior is observed for different alloy compositions of the stressor.

The strain data is then used as input in the $\mathbf{k}\cdot\mathbf{p}$ model to calculate the band energies over the cross section. Figure 3 shows the profiles of the conduction and valance band structures. To better understand the band structure shift due to the strained configuration, we derive the band edges across the middle slice of the cross section. Figure 4 depicts the conduction and valence bands along the $y = 25$ nm ray. The valence bands are clearly separated and based on the strain profile the heavy hole band has larger energy than the light holes, with the split-off band being at the lowest energy level.

IV. Summary and Outlook

We modelled and simulated non-linear strain in bent hexagonal-type nanowires to study its influence on the band edge energies. Notice that the valence edge bands do not cross; this enables us to easily identify which band corresponds to holes and is helpful for future drift-diffusion simulations which in turn can be used for comparisons with experiments.

Acknowledgment

This work is supported by the Leibniz association & DFG under Germany's Excellence Strategy EXC2046: MATH+ Berlin Mathematics Research Center (Project IN-7, O.M.). The authors thank C. Manganelli, M. Liero, & O. Brandt.

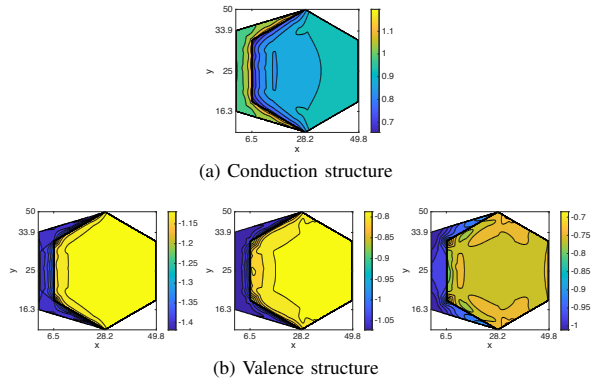

(a) Conduction structure

(b) Valence structure

Fig. 3. Surface plots of conduction band (top panel) and valence bands (bottom panel) across the cross section plane.

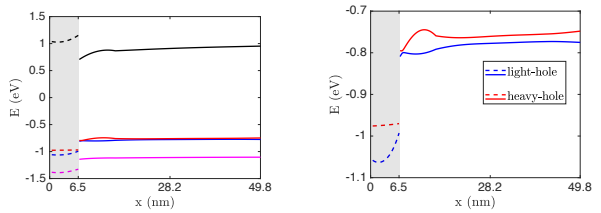

(a) *Left*: Conduction and valence bands. *Right*: Close-up of valence bands

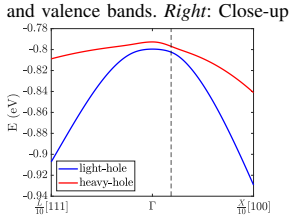

(b) Valence bands vs k.

Fig. 4. *Top panel*: Band structures at the Γ point along the middle slice in x-direction (i.e., at $y = 25$ nm). The gray area denotes the stressor region. *Bottom panel*: Band structures with respect to the norm k of the wave functions at the point $(x, y) = (8\text{ nm}, 25\text{ nm})$ (located in the core region). The dotted vertical line corresponds to the wave function for which the difference between the valence bands is minimum.

References

[1] K. M., Brendan, H. A. Atwater, and N. S. Lewis, "Comparison of the device physics principles of planar and radial p-n junction nanorod solar cells", J App. Phys. vol. 97(11), pp. 114302 (2005).

[2] Lewis, Ryan B., Pierre Corfdir, Hanno Küpers, Timur Flissikowski, Oliver Brandt, and Lutz Geelhaar, "Nanowires bending over backward from strain partitioning in asymmetric core-shell heterostructures", Nano Lett vol.18(4), pp. 2343-2350 (2018).

[3] Vurgaftman, Igor and Meyer-Arendt, Jurgen R., and Ram-Mohan, L. Ramdas, "Band parameters for III–V compound semiconductors and their alloys", J App. Phys. vol. 89(11), pp. 5815-5875 (2001).

[4] Marquardt, O., Schulz S., Freysoldt C., Boeck S., Hickel T., O'Reilly E. P., Neugebauer J., "A flexible, plane-wave based k·p multiband model", Opt Quant Electron vol. 44(3), pp. 183-188 (2012).

[5] Enders, P., A. Bärwolff, M. Woerner, and D. Suisky, "k·p theory of energy bands, wave functions, and optical selection rules in strained tetrahedral semiconductors", Phys Rev B, vol. 51(23), pp. 16695 (1995).

[6] Ciarlet, P. G., "Mathematical elasticity: Three-dimensional elasticity", Elsevier, vol. 1 (1988).